THE JOURNAL OF PHYSICAL CHEMISTRY A

Article

pubs.acs.org/JPCA

Evaluation of Hybrid Theoretical Approaches for Structural Determination of a Glycine-Linked Cisplatin Derivative via Infrared Multiple Photon Dissociation (IRMPD) Action Spectroscopy

C. C. He,[†] B. Kimutai,[†] X. Bao,[†] L. Hamlow,[†] Y. Zhu,[†] S. F. Strobehn,[†] J. Gao,[‡] G. Berden,[‡] J. Oomens,[‡,§] C. S. Chow,[†] and M. T. Rodgers*[,†]

[†]Department of Chemistry, Wayne State University, Detroit, Michigan 48202, United States

[‡]FELIX Laboratory, Institute for Molecules and Materials, Radboud University, Toernooiveld 7c, 6525ED Nijmegen, The Netherlands

[§]van't Hoff Institute for Molecular Sciences, University of Amsterdam, 1090 GD Amsterdam, The Netherlands

Supporting Information

ABSTRACT: To gain a better understanding of the binding mechanism and assist in the optimization of chemical probing and drug design applications, experimental and theoretical studies of a series of amino acid-linked cisplatin derivatives are being pursued. Glyplatin (glycine-linked cisplatin) was chosen for its structural simplicity and to enable backbone effects to be separated from side-chain effects on the structure and reactivity of ornithine- and lysine-linked cisplatin (Ornplatin and Lysplatin, respectively). Infrared multiple photon dissociation (IRMPD) action spectroscopy experiments were performed on Glyplatin to characterize its structure and guide the selection of the most effective hybrid theoretical approach for determining its structure and IR spectrum. The simplicity of the Glyplatin system allows a wide variety of density functionals, treatments of the Pt center including the use of all-electron basis sets vs valence basis sets combined with an effective core potential (ECP), and basis sets for all other atoms to be evaluated at a reasonable computational cost. The results for Glyplatin provide the foundation for calculations of more complex amino acid-linked cisplatin derivatives such as Ornplatin and Lysplatin. Present results suggest that the B3LYP/mDZP/def2-TZVP hybrid method can be effectively employed for structural and IR characterization of more complex amino acid-linked cisplatin complexes and their nucleic acid derivatives.

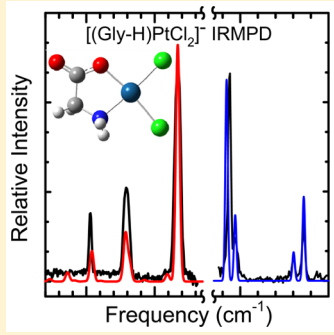

INTRODUCTION

The first FDA-approved platinum-based anticancer drug, cisplatin (Figure 1), has been widely used in cancer chemotherapy, particularly for testicular and ovarian cancers.[1] The pharmacological mechanism of cisplatin is associated with its ability to coordinate to genomic DNA, and in particular, guanine (G) residues.[2] Despite its success, cisplatin exhibits several drawbacks including increasing resistance and severe side effects, which are often associated with the variable repair mechanisms of nuclear DNA and off-target effects on the cytoplasmic components.[1,3] Recent studies have demonstrated that cisplatin accumulates faster and is more highly retained on RNA compared to DNA.[4] The reactivity of cisplatin toward RNA may cause general damage to RNA structure and potentially impact the established DNA-based mechanism.[5,6] As a result, the development of RNA-targeting Pt compounds is one of the approaches being pursued to overcome DNA repair-related resistance and reduce dose-related side effects. In a previous report, cisplatin was successfully utilized as a chemical probe to detect solvent accessible sites in ribosomal RNA (rRNA).[7] Amino acid-linked derivatives were developed to alter the reactivity and potentially selectively bind to sites other than guanine residues.[8] The probing results provided valuable structural information about rRNA and showed that the reactivity of Pt(II) complexes can be altered with modifications to the size and charge distribution within the complex. Among the amino acid-linked cisplatin derivatives, Ornplatin (ornithine-linked cisplatin) has demonstrated an unambiguous and template-independent binding preference for adenine (A) residues, particularly those in single-stranded regions, making

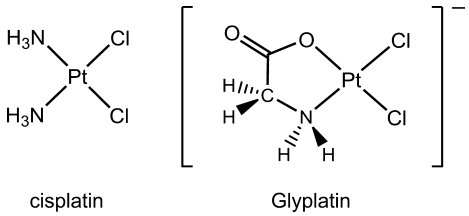

Figure 1. Structures of cisplatin and Glyplatin.

Received: August 22, 2015
Revised: October 16, 2015
Published: October 16, 2015

DOI: 10.1021/acs.jpca.5b08181
J. Phys. Chem. A 2015, 119, 10980−10987

it the first Pt(II) complex reported that exhibits selectivity for A over G.

Rational drug design is difficult, as an understanding of the structure−activity relationship is generally poor and only elucidated through exhaustive studies. Thousands of novel Pt-based antitumor drugs have been synthesized and screened for improved biological activity, yet only a few have succeeded.[9−11] In order to lay the foundation for intelligent drug design, several gas-phase spectroscopic studies have been performed to characterize the structures of Pt-based antitumor drugs including monoaquated cisplatin and its purine and DNA adducts.[12−14] Lippard and co-workers have made valuable contributions to the understanding of how cisplatin reacts with DNA. They proposed a theory that explains the preference of cisplatin for guanine[15] and also evaluated the effects of N7 platination of guanine on the stability of the glycosidic bond.[16] Lysplatin (lysine-linked cisplatin) has also been reported to be a promising anticancer drug based on their biochemistry study, where a binding mode involving (N,O) chelation of Lys has been proposed in the condensed phase.[17,18] Therefore, detailed calculations are needed to reveal the structures and mechanisms of the reactivity of amino acid-linked cisplatin analogues.

Systematic studies of theoretical methods and basis set selection have been performed for cisplatin and compared to condensed phase results.[19−23] All-electron basis sets with a new contraction scheme have recently been developed for platinum[23−25] but have not yet been examined for spectroscopic characterization of cisplatin and its derivatives. Because of potential differences between cisplatin and its amino acid-linked analogues in the condensed and gas phases, the best choice of theoretical methods must be validated via comparison with spectroscopic results. Due to its structural simplicity and lack of a floppy side chain, Glyplatin (glycine-linked cisplatin, $[(\text{Gly-H})\text{PtCl}_2]^-$, Figure 1) provides an opportunity for a wide variety of hybrid theoretical approaches to be evaluated at a reasonable computational cost. Infrared multiple photon dissociation (IRMPD) action spectroscopy is an effective approach for the study of the structures of gas-phase ions.[26] By use of a combination of the IRMPD and theoretical techniques, the structure of Glyplatin is elucidated via comparison of the measured IRMPD and computed IR spectra for the stable structures computed. The fidelity with which each hybrid theoretical approach is able to reproduce the measured IRMPD spectrum is evaluated to determine the most accurate and efficient approaches for theoretically characterizing the structures and IR spectra of Pt(II) based complexes.

EXPERIMENTAL AND COMPUTATIONAL APPROACHES

Experimental Protocols. The IRMPD action spectrum of Glyplatin was measured using a 4.7 T Fourier transform ion cyclotron resonance mass spectrometer (FT-ICR MS).[27−29] Glyplatin was synthesized and purified using procedures reported previously.[30] Glyplatin ions, $[(\text{Gly-H})\text{PtCl}_2]^-$, were generated using a Micromass "Z-spray" electrospray ionization (ESI) source from solutions containing ∼1−7 mM Glyplatin in a 50:50 (v/v) MeOH/H_2O mixture. The solution was sprayed at a flow rate of ∼2 μL/min, and the voltage on the ESI needle was held at −2.5 kV. Ions emanating from the spray were guided and accumulated in an rf hexapole ion trap for 5.5−12.5 s to provide an intense ion signal and ensure efficient thermalization of the ions. Ions were pulse extracted through a quadrupole bender and injected into the ICR cell by an rf octopole ion guide. Glyplatin ions, $[(\text{Gly-H})\text{PtCl}_2]^-$, were mass selected and isolated using stored waveform inverse Fourier transform (SWIFT) techniques in the ICR cell. Spectral data in the fingerprint region were acquired by coupling the FT-ICR MS to the widely tunable free-electron laser for infrared experiments (FELIX), which provides pulse energies of up to 40 mJ per 5 μs pulse, at a 5 Hz repetition rate, and a bandwidth of 0.5% of the laser frequency.[31] Ions were irradiated for 4 s by the free-electron laser over the frequency range extending from 585 to 1820 cm^{-1}. To obtain spectral data in the hydrogen-stretching region, 2900−3700 cm^{-1}, the FT-ICR MS instrument was coupled to a Nd:YAG-pumped (Innolas Spitlight 600) optical parametric oscillator laser system (OPO, LaserVision, Bellevue, WA). Ions were irradiated for 11 s by the OPO laser, which provides 6 ns pulses at a 10 Hz repetition rate with energies of up to 20 mJ and a bandwidth of 3 cm^{-1}. Due to the lack of strong hydrogen-stretching vibrations, the ions were irradiated for 50 ms with the output of a 30 W continuous wave CO_2 laser directly after each OPO pulse to facilitate dissociation of the resonantly excited ions.[32] The IR laser frequency is calibrated using a grating spectrometer for the free-electron laser and a wavemeter (HighFinesse GmbH, Germany) for the OPO laser.

Three mass spectra were averaged and recorded at each laser frequency. The IRMPD yield was calculated from the ratio of the sum of the intensities of all fragment ions versus the total ion intensity, IRMPD yield = $\sum I_{f_i}/(\sum I_{f_i} + I_p)$, where I_{f_i} and I_p are the ion intensities of the fragment and precursor ions, respectively. The IRMPD yield was linearly corrected for the frequency dependent variations of the free-electron laser (FEL) pulse energy or OPO laser pulse energy in their corresponding regions and plotted as a function of infrared frequency to produce the IRMPD spectrum.

Computational Protocols. All theoretical calculations were performed using Gaussian 09.[33] Basis sets that are not incorporated in the Gaussian software were acquired from the EMSL basis set exchange library.[34,35] For all theoretical spectra, scaling factors were used to correct for the differences between experimental and theoretical spectra to eliminate known systematic errors, which are caused by the neglect of anharmonicity, the incomplete incorporation of electron correlation, and the use of finite basis sets.[36,37] Results in the fingerprint region (measured using the FEL) were aligned to the C═O stretch at 1669 cm^{-1}. Scaling factors that vary from 0.9283 to 0.9881 were applied along with convolution over a Gaussian shape having a fwhm of 20 cm^{-1} to simulate the experimental spectrum. All theoretical data in the hydrogen-stretching region were aligned to the NH_2 asymmetric stretch at 3360 cm^{-1}. Scaling factors that vary from 0.9321 to 0.9823 were applied along with convolution over a Gaussian shape having a fwhm of 10 cm^{-1}. The scaling factors (SF) used for each hybrid theoretical approach are listed in Table S1 in Supporting Information.

In this study, we evaluate a variety of hybrid theoretical approaches for the characterization of Glyplatin and related amino acid-linked cisplatin derivatives based on the density functional, treatment of the Pt center, and basis set used to describe the remainder of the system. A total of seven different density functionals including B3LYP, B3PW91, mPW1PW91, M06, PBE0, LC-ωPBE, and CAM-B3LYP were chosen for examination based on previous studies of cisplatin. In particular, previous studies have suggested that several of these DFT

DOI: 10.1021/acs.jpca.5b08181
J. Phys. Chem. A 2015, 119, 10980−10987

methods exhibit better performance than B3LYP,[19−23] and thus these conclusions are re-examined here for Glyplatin. The challenge associated with describing the Pt center is due to the large number of electrons it possesses. Five valence basis sets along with their corresponding ECPs including LANL2DZ, LANL2TZ, LANL2TZ(f), SDD, and def2-TZVP were examined and are compared to three all-electron basis sets including the recently developed all-electron double-ζ polarization basis set (DZP) and its augmented derivatives (ADZP and mDZP). Nineteen different basis sets were examined for the nonmetal atoms including eight Pople, six Dunning, and five Ahlrichs basis sets. Details regarding the choice of basis sets employed are summarized in Table 1. As illustrated in the table,

Table 1. Basis Sets Used for Nonmetal Atoms of $[(Gly\text{-}H)PtCl_2]^-$

type	Pople	Dunning	Ahlrichs
double ζ	6-31G	cc-pVDZ	def2-SVP
	6-31G(d)	aug-cc-pVDZ	
	6-31+G(d)		
	6-31+G(d,p)		
triple ζ	6-311+G(d,p)	cc-pVTZ	def2-TZVP
	6-311++G(d,p)	aug-cc-pVTZ	def2-TZVPPD
	6-311+G(2d,2p)		
	6-311+G(3df,3dp)		
quadruple ζ		cc-pVQZ	def2-QZVP
		aug-cc-pVQZ	def2-QZVPPD

the sizes of the basis sets were carefully increased in each series to examine the effects of the flexibility (ζ), polarization functions, and diffuse functions on the computed IR spectra. To provide a consistent treatment of Pt and the other atoms comprising Glyplatin, four Ahlrichs basis sets (def2-TZVP, def2-QZVP, def2-TZVPPD, and def2-QZVPPD) and two all-electron basis sets (DZP and ADZP) were also used to describe all atoms. Henceforth, the hybrid theoretical approaches examined will be abbreviated as follows: DFT method/Pt treatment/nonmetal atom basis set. To provide a quantitative assessment of the theoretical results, the mean absolute error (MAE, in cm^{-1}) between the measured and computed frequencies of the seven major features was calculated for each theoretical approach.[22,38] The measured frequencies are compared to the predicted frequencies in Table S2, which also lists the deviations between the measured and computed frequencies and the MAE for each hybrid theoretical approach.

Finally, anharmonic calculations were also performed using second-order vibrational perturbation theory (VPT2) implemented in Gaussian 09.[33,39] Due to the difficulty of combining the all-electron basis set (mDZP) into the anharmonic calculation, the B3LYP/LANL2TZ(f)/def2-TZVP approach was examined in these comparisons. The deperturbed and generalized VPT2 approaches (DVPT2 and GVPT2) as well as the degeneracy-corrected PT2 approach (DCPT2) were examined. Because vibrational spectroscopic analysis is not available for DCPT2 in the version of Gaussian 09 available, the frequencies were taken from vibrational energies and combined with the corresponding anharmonic intensities based on the GVPT2 method to generate the convoluted DCPT2 spectrum.

RESULTS AND DISCUSSION

When the ions were irradiated with the free-electron laser, both HCl loss and a combination of HCl and CO_2 loss were observed. However, when the ions were fragmented in the hydrogen-stretching region, only HCl loss was observed. To first determine the ground-state structure of Glyplatin, calculations were performed at the B3LYP/def2-TZVPPD level of theory using the corresponding valence basis set and effective core potential (ECP) for Pt. Eight local minimum structures were found, and their IR spectra compared to the experimental IRMPD spectrum of Glyplatin in Figure 2 and

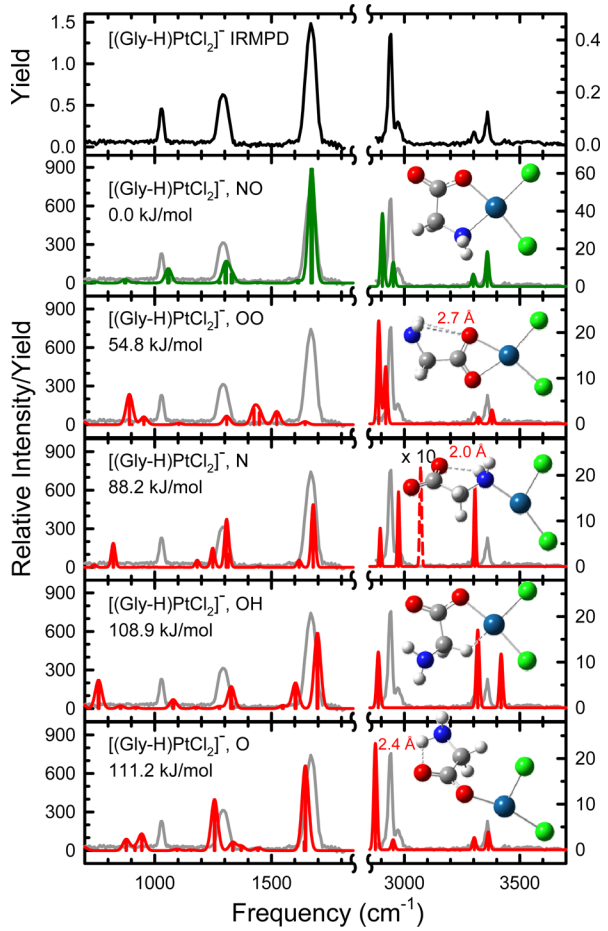

Figure 2. Comparison between the experimental IRMPD spectrum and calculated IR spectra predicted for the five stable binding modes of $[(Gly\text{-}H)PtCl_2]^-$: NO, OO, N, OH, and O. The corresponding B3LYP/def2-TZVPPD optimized structures and relative Gibbs free energies at 298 K are also included.

Figure S1. Scaling factors of 0.98 were applied to all computed spectra in the fingerprint region of 700−1850 cm^{-1} and 0.95 in the hydrogen-stretching region of 2850−3700 cm^{-1}, to compensate for known systematic errors in the calculated frequencies. The B3LYP/def2-TZVPPD method and basis set were chosen based on previous studies, which found that this level of theory produces a satisfactory description of the band positions and bond dissociation energies of complexes involving metal cations.[40,41] The stable structures found for $[(Gly\text{-}H)PtCl_2]^-$ are designated by their modes of binding to the Pt center (see Figure 2). NO binding indicates that Pt is chelated to the backbone amino nitrogen and one of the carboxylate oxygen atoms. OO binding indicates bidentate binding to Pt via both oxygen atoms of the carboxylate moiety. N binding indicates monodentate binding to Pt via the backbone amino nitrogen atom. OH binding indicates

DOI: 10.1021/acs.jpca.5b08181
J. Phys. Chem. A 2015, 119, 10980−10987

bidentate binding via interaction with one of the carboxylate oxygen atoms and one of the α-carbon hydrogen atoms. O binding indicates monodentate interaction with one of the carboxylate oxygen atoms. Structures involving the deprotonated backbone amino nitrogen and neutral carboxylic acid moiety were also examined. Different proton orientations and positions on the carboxylic acid moiety were considered (Figure S1). However, all three structures are much higher (by >130 kJ/mol) in relative Gibbs free energy than the NO binding structure. Hence, deprotonation of the backbone amino nitrogen is ruled out. Among the eight stable structures found, the IR spectrum predicted for the NO binding structure of $[(Gly\text{-}H)PtCl_2]^-$ is the only predicted spectrum that provides a good match to the measured IRMPD spectrum indicating that the NO binding mode is the only structure populated in the experiments. This NO binding mode is also consistent with the structures reported for Ornplatin[42] and Lysplatin[17] in the condensed phase and suggests that Glyplatin may serve as a reliable model for other amino acid-linked cisplatin derivatives. Shifts in the positions of the bands vs the measured spectrum indicate that the B3LYP/def2-TZVPPD level of theory is not able to reproduce the IRMPD spectrum with high fidelity. On the basis of this preliminary structural determination, all further calculations were performed for the complex involving the NO mode of binding.

Peak assignments based on the theoretical results indicate that the dominant peak in the experimental spectrum arises from C═O stretching at a frequency of 1669 cm^{-1}. The second most intense peak is contributed by C−O stretching and CH_2 wagging at 1294 cm^{-1}, with contributions from CH_2 wagging and NH_2 twisting at 1325 cm^{-1}. The peak at ∼1030 cm^{-1} arises from NH_2 wagging. In the hydrogen-stretching region, the CH_2 symmetric stretch is the strongest band and appears at 2939 cm^{-1}, whereas the CH_2 asymmetric stretch appears at 2972 cm^{-1}. NH_2 symmetric and asymmetric stretches appear at 3302 and 3360 cm^{-1}, respectively. Details regarding the vibrational band assignments are listed in Table 2. Blue shifts of the bands at 1030 and 1577 cm^{-1} are observed as well as red shifts of the features in the hydrogen-stretching region, particularly for the band at 2939 cm^{-1}. The lack of peak alignment throughout the IR region indicates the importance of choosing the density functional, treatment of the Pt center, and basis set for nonmetal atoms carefully to accurately describe the binding in amino acid-linked cisplatin complexes.

Different treatments for the nonmetal atoms were evaluated first. Pople basis sets that increase from 6-31G to 6-311+(3df,3dp), Dunning basis sets from cc-pVDZ to aug-cc-pVQZ, as well as Ahlrichs basis sets from def2-SVP to def2-QZVPPD were examined in conjunction with the B3LYP method and the LANL2DZ valence basis set and ECP for Pt.[33−35] The IR spectral results are compared in Figures 3 and 4. All theoretical spectra were aligned to the strong C═O stretch in the fingerprint region (irradiated with the FEL) and the NH_2 asymmetric stretch in the hydrogen-stretching region (irradiated with the OPO laser system). Details regarding the basis set and corresponding scaling factors used are listed in Table S1, whereas the computed frequencies, differences in the measured and computed frequencies, and MAEs are summarized in Table S2 of the Supporting Information. Theoretical results for the Pople basis sets in the fingerprint region are compared in Figure 3a. The 6-31G basis set does not provide very satisfying results (MAE = 22.4 cm^{-1}). An increase in the size of the basis set to 6-31G(d) significantly improves the predicted spectrum (MAE = 11.4 cm^{-1}), indicating that the extra polarization function is essential for these calculations. Use of the 6-31+G(d) basis set improves the prediction of the band at 1294 cm^{-1}; however, this basis set exhibits poorer prediction of the feature at ∼1030 cm^{-1}. Overall, the MAE values are similar for 6-31G(d) and 6-31+G(d), indicating that the additional diffuse function does not necessarily lead to better results. Addition of a polarization function on the hydrogen atoms, corresponding to the 6-31+G(d,p) basis set, improves predictions in the fingerprint region significantly; however, the overall MAE value is actually worse than the smaller 6-31G(d) and 6-31+G(d) basis sets. Increases in the basis set beyond 6-31+G(d,p) such as 6-311+G(d,p), 6-311++G(d,p), and

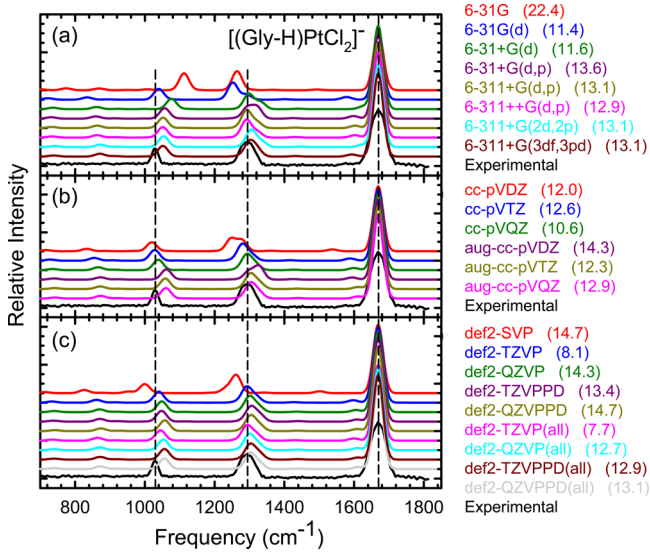

Figure 3. Comparison between the experimental IRMPD spectrum and B3LYP IR spectra predicted using (a) Pople, (b) Dunning, and (c) Ahlrichs basis sets for the nonmetal atoms of $[(Gly\text{-}H)PtCl_2]^-$ in the fingerprint region. Pt was treated using the LANL2DZ valence basis set with its corresponding ECP in all calculations except when the four Ahlrichs basis sets were used and all atoms were treated using the same basis set. MAE values are listed in the parentheses.

Table 2. Vibrational Band Assignments for $[(Gly\text{-}H)PtCl_2]^-$ [a]

experimental (cm^{-1})[b]	vibrational mode assigned	B3LYP/def2-TZVPPD predicted frequency (cm^{-1})[c]
1030(4)	NH_2 wagging	1056 (26)
1294(2)	C−O$^-$ stretching/CH_2 wagging	1302 (8)
1325(2)	CH_2 wagging/NH_2 twisting	1328 (3)
1577(5)	NH_2 bending	1611 (34)
1669(6)	C═O stretching	1669 (0)
2939(1)	CH_2 symmetrical stretching	2906 (33)
2972(1)	CH_2 asymmetrical stretching	2952 (20)
3302(2)	NH_2 symmetrical stretching	3299 (3)
3360(1)	NH_2 asymmetrical stretching	3360 (0)

[a]Scaling factors of 0.9781 and 0.9502 were used in the fingerprint and hydrogen-stretching regions, respectively. [b]Uncertainties are indicated in parentheses. [c]Shifts in the predicted frequencies vs the measured values are listed in parentheses.

DOI: 10.1021/acs.jpca.5b08181
J. Phys. Chem. A 2015, 119, 10980−10987

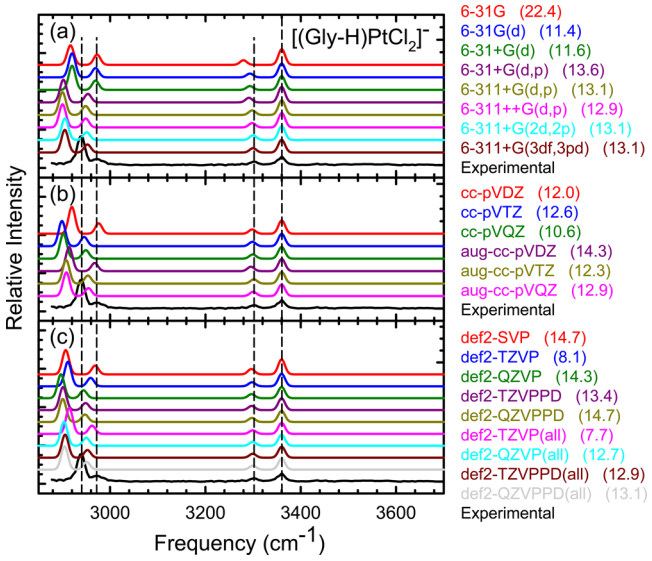

Figure 4. Comparison between the experimental IRMPD spectrum and B3LYP IR spectra predicted using (a) Pople, (b) Dunning, and (c) Ahlrichs basis sets for the nonmetal atoms of $[(Gly\text{-}H)PtCl_2]^-$ in the hydrogen-stretching region. Pt was treated using the LANL2DZ valence basis set with its corresponding ECP in all calculations except when the four Ahlrichs basis sets were used and all atoms were treated with the same basis set. MAE values are listed in the parentheses.

6-311+G(3df,3pd) produce only small differences and even lead to slightly poorer agreement for the 6-311+G(2d,2p) basis set in the fingerprint region. In the hydrogen-stretching region (see Figure 4a), each Pople basis set exhibits its own limitations. Additional polarization functions on the hydrogen atoms doesn't improve the prediction of the N−H stretch significantly, and degrades that for the C−H stretch. These results indicate that adding additional polarization and diffuse functions to the nonmetal atoms does not improve the results beyond the 6-31+G(d) basis set in the hydrogen-stretching region. Overall, none of the Pople basis set gives a satisfactory result in both regions. 6-31G(d) seems to be acceptable based on its low cost and relatively good performance, even though the shift around 1294 cm^{-1} is quite significant (42 cm^{-1}).

Among the Dunning basis sets (see Figure 3b), correlation consistent results in the fingerprint region improve with the increasing flexibility provided by the additional (ζ) orbital exponents. In comparison, the performance of augmented basis sets is slightly worse in the fingerprint region. In the hydrogen-stretching region (Figure 4b), the augmented basis sets improve the predictions for C−H stretching. Overall, cc-pVQZ provides the most accurate prediction among the Dunning basis sets (MAE = 10.6 cm^{-1}). For the Ahlrichs basis sets (Figure 3c and Figure 4c), results from consistent Ahlrichs treatments and LANL2DZ of Pt are compared because previous work has indicated that def2-TZVPPD with the corresponding ECP for Pt generally provides the best results for heavy metal systems.[40,41] It is clear that the def2-TZVP basis set provides the best results when combined with the LANL2DZ treatment for Pt among this series (MAE = 8.1 cm^{-1}). Similar to the Pople basis sets, the addition of polarization or diffuse functions does not significantly improve the accuracy of the theoretical description. The def2-TZVP basis set provides better results than all of the Pople basis sets examined but provides a poor description of the C−H stretching modes. Because of its outstanding performance and low cost, the def2-TZVP basis was chosen as the optimal basis set for the nonmetal atoms. The very good performance of the def2-TZVP basis set may result from the relatively balanced treatment of the metal center and nonmetal atoms. To further confirm this assumption, the four Ahlrichs basis sets were used for all atoms and compared (Figure 3c and Figure 4c). Among these results, the def2-TZVP basis set provides the best prediction of the IR spectrum, which is also better than results based on the LANL2DZ valence basis set and ECP treatment for Pt. These results also indicate that the treatment of the Pt center must be chosen very carefully.

The treatment of the Pt(II) metal center of cisplatin and its amino acid-linked analogues is challenging due to the large number of electrons and the non-negligible relativistic effects of the third transition row. To overcome this limit, calculations on Pt complexes such as cisplatin and its derivatives are normally performed with a suitable valence basis set combined with an effective core potential for the Pt(II) center. However, basis sets have yet to be validated for amino acid-linked Pt(II)-based complexes. In the present work, five valence basis sets and ECP treatments are compared with three all-electron basis sets in Figure 5. Previous theoretical studies on cisplatin indicated that

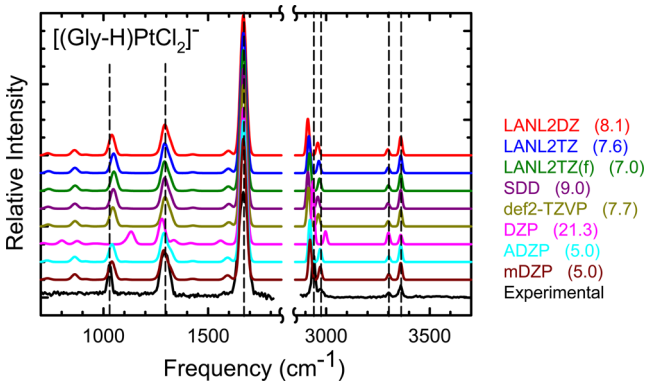

Figure 5. Comparison between the experimental IRMPD spectrum and B3LYP/Pt treatment/def2-TZVP IR spectra predicted for $[(Gly\text{-}H)PtCl_2]^-$ for various treatments of the Pt center. MAE values are listed in the parentheses.

LANL2DZ (with the Hay and Wadt ECP) is a reasonable choice for cisplatin calculations.[19] The addition of a ζ set [from LANL2DZ to LANL2TZ] or a polarization function [from LANL2TZ to LANL2TZ(f)] improves the overall computed frequencies (MAEs of 8.1, 7.6, and 7.0 cm^{-1}, respectively), consistent with previous work reported in the literature.[22] Although the Stuttgart−Dresden ECP (SDD) treatment provides a better description than LANL2DZ for many transition metal complexes, slightly poorer agreement is found here for Glyplatin (MAE = 9.0 cm^{-1}). The def2-TZVP treatment was again employed to achieve size consistency with the nonmetal atoms. The def2-TZVP treatment (MAE = 7.7 cm^{-1}) provides results similar to those from LANL2TZ, slightly worse than LANL2TZ(f) but better than all other ECP treatments. Among the all-electron basis sets examined, ADZP and mDZP (modified DZP) provide similar and reliable results when combined with the def2-TZVP basis set for the nonmetal atoms (MAEs of 5.0 cm^{-1}). These approaches also provide an improved description of the NH_2-wagging in the fingerprint region and the C−H stretches in the hydrogen-stretching region as compared to LANL2TZ(f) and def2-TZVP. Because

DOI: 10.1021/acs.jpca.5b08181
J. Phys. Chem. A 2015, 119, 10980−10987

of its smaller size relative to ADZP, mDZP was selected for further study. For the all-electron basis set treatments, the DZP and augmented DZP (ADZP) basis sets are also available for all nonmetal atoms. Thus, B3LYP calculations were also performed using these basis sets for all atoms for the purpose of size consistency, but the results are poor (MAEs of 26.7 and 15.1 cm^{-1}; also see Figure S2 of the Supporting Information). In summary, the mDZP all-electron basis set for Pt combined with the def2-TZVP basis set for the nonmetal atoms yields the best results with the B3LYP functional.

DFT methods are widely applied due to their relatively low cost and acceptable results for many systems. As our goal is to determine the most efficient method and basis set for calculations on other amino acid-linked cisplatin analogues, only DFT methods were examined and compared in the present work. B3LYP is often the method of choice because of the benefit of its three-parameter hybridization.[43,44] B3PW91 and mPW1PW91 have been reported to provide good agreement with experiments for cisplatin and thus are also examined.[19−23] M06 was also included given its good performance in studies of transition metal−ligand interactions.[45] PBE0 and LC-ωPBE are also examined based on previous results for cisplatin.[22] CAM-B3LYP, as a further optimized B3LYP method, was also included. Figure 6 indicates

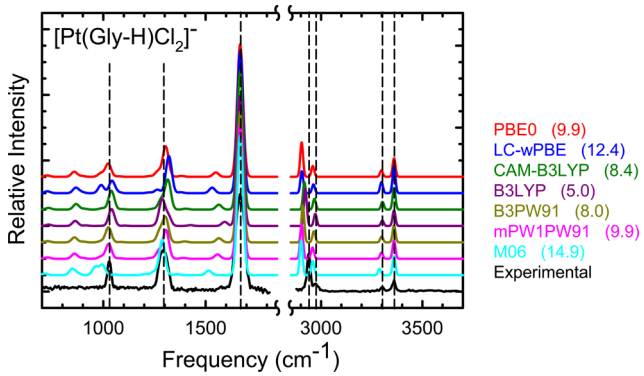

Figure 6. Comparison between the experimental IRMPD spectrum and the IR spectra predicted for $[(Gly\text{-}H)PtCl_2]^-$ using various DFT methods along with the mDZP and def2-TZVP basis sets to describe Pt and all other atoms, respectively. MAE values are listed in the parentheses.

that even though PBE0 and LC-ωPBE were recommended for computing vibrational spectra based on a previous study of cisplatin, these methods do not provide results that are as satisfying as the B3LYP method for Glyplatin (MAEs of 9.9 and 12.4 cm^{-1} vs 5.0 cm^{-1}). CAM-B3LYP gives results highly parallel to those of B3LYP. However, detailed band position comparisons find that CAM-B3LYP performs slightly worse (MAE = 8.4 cm^{-1}) than B3LYP. It is also clear that M06 provides the least reliable prediction for the geometry of Glyplatin among the density functionals examined here (MAE = 14.9 cm^{-1}). B3PW91 and mPW1PW91 provide slightly poorer predictions (MAEs of 8.0 and 9.9 cm^{-1}) than B3LYP, besides their slightly higher computational cost. Hence, B3LYP is found to be the most suitable DFT method for further calculations.

The measured IRMPD spectrum is compared to the B3LYP/LANL2TZ(f)/def2-TZVP IR spectra predicted based on the anharmonic and harmonic approaches examined in Figure S3. Variations in the predicted spectra, particularly in the hydrogen-stretching region, suggest that the differences between the experimental and predicted spectra are primarily due to anharmonic effects. Unfortunately, all three anharmonic approaches available in Gaussian 09 are unable to provide improved descriptions of the IR spectrum of Glyplatin in the hydrogen-stretching region vs those based on the simpler harmonic approximation. To achieve more accurate spectral predictions, more advanced and computationally intensive approaches for the treatment of anharmonicity are being developed and pursued by several theoretical research groups.[46,47] As the goal of the present work is to determine the most efficient hybrid theoretical approaches for the characterization of Glyplatin and more complex amino acid-linked cisplatin derivatives, detailed time-consuming anharmonic calculations are left to the experts.

CONCLUSIONS

Balanced basis sets for platinum and the nonmetal atoms of Glyplatin provide the most reasonable results. The B3LYP/mDZP/def2-TZVP approach provides a robust description of the vibrational spectrum of Glyplatin. However, if large platinum-biomolecular complexes are of interest, their ground-state structures may not be easily identified, may require more comprehensive searching for stable structures, and even mapping of the potential energy surface may be necessary. In such cases, use of the 6-31G(d) basis set for the treatment of nonmetal atoms is recommended due to its ability to produce relatively good results at a low computational cost. If the fingerprint region spectrum is more congested such as expected for more complex amino acid-linked cisplatin derivatives, the 6-31+G(d,p) basis set is recommended. Herein, the B3LYP/mDZP/def2-TZVP method is recommended for future calculations of amino acid-linked cisplatin derivatives. It is important to note that this approach is chosen based on the accurate prediction of geometric information for Glyplatin and may not represent the best choice for energetic predictions. Comparison between the methods and basis sets evaluated and recommended for cisplatin (a neutral complex) and the best results found here for Glyplatin (a negatively charged complex) suggests that the best hybrid theoretical approach may be influenced by the overall charge of the complex. This observation will be examined further in future studies of the $[(Orn)PtCl]^+$ and $[(Lys)PtCl]^+$ complex ions that are readily produced by ESI of the neutral Ornplatin and Lysplatin complexes.

ASSOCIATED CONTENT

Supporting Information

The Supporting Information is available free of charge on the ACS Publications website at DOI: 10.1021/acs.jpca.5b08181.

Complete citation for ref 33; tables of scaling factors used to align the predicted IR spectra of Glyplatin with the measured IRMPD spectrum and the measured and predicted frequencies along with the deviations in these values and calculated mean absolute errors (MAEs, in cm^{-1}); figures comparing the measured IRMPD spectrum with IR spectra predicted for structures involving deprotonation of the backbone amino moiety, those using the DZP and ADZP basis sets for all atoms, and those determined using harmonic vs anharmonic approaches to predict the IR spectra. (PDF)

DOI: 10.1021/acs.jpca.5b08181
J. Phys. Chem. A 2015, 119, 10980−10987

AUTHOR INFORMATION

Corresponding Author

*Phone: 313 577-2431. E-mail: mrodgers@chem.wayne.edu.

Notes

The authors declare no competing financial interest.

ACKNOWLEDGMENTS

This work is financially supported by the National Science Foundation, under Grants OISE-0730072 and CHM-1409420, the National Institutes of Health (Grant GM087596), and a Paul A. Schaap Faculty Fellowship. We thank Wayne State University C&IT for the computational resources and support. We also thank Dr. Jun Jiang and Dr. Claudio N. Verani for technical advice. This work is part of the research program of FOM, which is financially supported by the Nederlandse Organisatie voor Wetenschappelijk Onderzoek (NWO). The skillful assistance of the FELIX staff is gratefully acknowledged.

REFERENCES

(1) Lippert, B. *Cisplatin: Chemistry and Biochemistry of a Leading Anticancer Drug*; Wiley-VCH: Weinheim, Germany, 1999; p 563.

(2) Jamieson, E. R.; Lippard, S. J. Structure, Recognition, and Processing of Cisplatin-DNA Adducts. *Chem. Rev.* **1999**, *99*, 2467−2498.

(3) Kelland, L. R.; Sharp, S. Y.; O'Neill, C. F.; Raynaud, F. I.; Beale, P. J.; Judson, I. R. Mini-Review: Discovery and Development of Platinum Complexes Designed to Circumvent Cisplatin Resistance. *J. Inorg. Biochem.* **1999**, *77*, 111−115.

(4) Hostetter, A. A.; Chapman, E. G.; DeRose, V. J. Rapid Cross-Linking of an RNA Internal Loop by the Anticancer Drug Cisplatin. *J. Am. Chem. Soc.* **2009**, *131*, 9250−9257.

(5) Chapman, E. G.; DeRose, V. J. Enzymatic Processing of Platinated RNAs. *J. Am. Chem. Soc.* **2010**, *132*, 1946−1952.

(6) Hostetter, A. A.; Osborn, M. F.; DeRose, V. J. RNA-Pt Adducts Following Cisplatin Treatment of Saccharomyces Cerevisiae. *ACS Chem. Biol.* **2012**, *7*, 218−225.

(7) Rijal, K.; Chow, C. S. A New Role for Cisplatin: Probing Ribosomal RNA Structure. *Chem. Commun.* **2009**, 107−109.

(8) Rijal, K.; Bao, X.; Chow, C. S. Amino Acid-Linked Platinum(II) Analogues Have Altered Specificity for RNA Compared to Cisplatin. *Chem. Commun.* **2014**, *50*, 3918−3920.

(9) Olszewski, U.; Hamilton, G. A Better Platinum-Based Anticancer Drug Yet to Come? *Anti-Cancer Agents Med. Chem.* **2010**, *10*, 293−301.

(10) Galanski, M. Recent Developments in the Field of Anticancer Platinum Complexes. *Recent Pat. Anti-Cancer Drug Discovery* **2006**, *1*, 285−295.

(11) Kostova, I. Platinum Complexes as Anticancer Agents. *Recent Pat. Anti-Cancer Drug Discovery* **2006**, *1*, 1−22.

(12) De Petris, A.; Ciavardini, A.; Coletti, C.; Re, N.; Chiavarino, B.; Crestoni, M. E.; Fornarini, S. Vibrational Signatures of the Naked Aqua Complexes from Platinum(II) Anticancer Drugs. *J. Phys. Chem. Lett.* **2013**, *4*, 3631−3635.

(13) Chiavarino, B.; Crestoni, M. E.; Fornarini, S.; Scuderi, D.; Salpin, J. Y. Interaction of Cisplatin with Adenine and Guanine: A Combined IRMPD, MS/MS, and Theoretical Study. *J. Am. Chem. Soc.* **2013**, *135*, 1445−1455.

(14) Chiavarino, B.; Crestoni, M. E.; Fornarini, S.; Scuderi, D.; Salpin, J. Y. Interaction of Cisplatin with 5′-dGMP: A Combined IRMPD and Theoretical Study. *Inorg. Chem.* **2015**, *54*, 3513−3522.

(15) Baik, M. H.; Friesner, R. A.; Lippard, S. J. Theoretical Study of Cisplatin Binding to Purine Bases: Why Does Cisplatin Prefer Guanine over Adenine? *J. Am. Chem. Soc.* **2003**, *125*, 14082−14092.

(16) Baik, M. H.; Friesner, R. A.; Lippard, S. J. Theoretical Study on the Stability of N-Glycosyl Bonds: Why Does N7-Platination Not Promote Depurination? *J. Am. Chem. Soc.* **2002**, *124*, 4495−4503.

(17) Sandman, K. E.; Fuhrmann, P.; Lippard, S. J. A Mechanism-Based, Solution-Phase Method for Screening Combinatorial Mixtures of Potential Platinum Anticancer Drugs. *JBIC, J. Biol. Inorg. Chem.* **1998**, *3*, 74−80.

(18) Ziegler, C. J.; Sandman, K. E.; Liang, C. H.; Lippard, S. J. Toxicity of Platinum(II) Amino Acid (N,O) Complexes Parallels Their Binding to DNA as Measured in a New Solid Phase Assay Involving a Fluorescent HMG1 Protein Construct Readout. *JBIC, J. Biol. Inorg. Chem.* **1999**, *4*, 402−411.

(19) Wysokinski, R.; Michalska, D. The Performance of Different Density Functional Methods in the Calculation of Molecular Structures and Vibrational Spectra of Platinum(II) Antitumor Drugs: Cisplatin and Carboplatin. *J. Comput. Chem.* **2001**, *22*, 901−912.

(20) Amado, A. M.; Fiuza, S. M.; Marques, M. P. M.; de Carvalho, L. A. E. B. Conformational and Vibrational Study of Platinum(II) Anticancer Drugs: Cis-Diamminedichloroplatinum(II) As a Case Study. *J. Chem. Phys.* **2007**, *127*, 185104.

(21) Fiuza, S. M.; Amado, A. M.; Marques, M. P. M.; de Carvalho, L. A. E. B. Use of Effective Core Potential Calculations for the Conformational and Vibrational Study of Platinum(II) Anticancer Drugs. Cis-Diamminedichloroplatinum(II) as a Case Study. *J. Phys. Chem. A* **2008**, *112*, 3253−3259.

(22) Malik, M.; Michalska, D. Assessment of New DFT Methods for Predicting Vibrational Spectra and Structure of Cisplatin: Which Density Functional Should We Choose for Studying Platinum(II) Complexes? *Spectrochim. Acta, Part A* **2014**, *125*, 431−439.

(23) Paschoal, D.; Marcial, B. L.; Lopes, J. F.; De Almeida, W. B.; Dos Santos, H. F. The Role of the Basis Set and the Level of Quantum Mechanical Theory in the Prediction of the Structure and Reactivity of Cisplatin. *J. Comput. Chem.* **2012**, *33*, 2292−2302.

(24) de Berredo, R. C.; Jorge, F. E. All-Electron Double Zeta Basis Sets for Platinum: Estimating Scalar Relativistic Effects on Platinum-(II) Anticancer Drugs. *J. Mol. Struct.: THEOCHEM* **2010**, *961*, 107−112.

(25) de Berredo, R. C.; Jorge, F. E.; Jorge, S. S.; Centoducatte, R. An Augmented Gaussian Basis Set for Calculations of Molecular Polarizabilities on Platinum Compounds. *Comput. Theor. Chem.* **2011**, *965*, 236−239.

(26) Oomens, J.; Sartakov, B. G.; Meijer, G.; Von Helden, G. Gas-Phase Infrared Multiple Photon Dissociation Spectroscopy of Mass-Selected Molecular Ions. *Int. J. Mass Spectrom.* **2006**, *254*, 1−19.

(27) Valle, J. J.; Eyler, J. R.; Oomens, J.; Moore, D. T.; van der Meer, A. F. G.; von Helden, G.; Meijer, G.; Hendrickson, C. L.; Marshall, A. G.; Blakney, G. T. Free Electron Laser-Fourier Transform Ion Cyclotron Resonance Mass Spectrometry Facility for Obtaining Infrared Multiphoton Dissociation Spectra of Gaseous Ions. *Rev. Sci. Instrum.* **2005**, *76*, 023103.

(28) Polfer, N. C.; Oomens, J.; Moore, D. T.; von Helden, G.; Meijer, G.; Dunbar, R. C. Infrared Spectroscopy of Phenylalanine Ag(I) and Zn(II) Complexes in the Gas Phase. *J. Am. Chem. Soc.* **2006**, *128*, 517−525.

(29) Polfer, N. C.; Oomens, J. Reaction Products in Mass Spectrometry Elucidated with Infrared Spectroscopy. *Phys. Chem. Chem. Phys.* **2007**, *9*, 3804−3817.

(30) Bao, X. Synthesis, Characterization, and RNA Reactivity of Amino-Acid-Linked Cisplatin Analogues. Ph.D. Dissertation, Wayne State University, Detroit, MI, January 2015.

(31) Oepts, D.; Vandermeer, A. F. G.; Vanamersfoort, P. W. The Free-Electron-Laser User Facility FELIX. *Infrared Phys. Technol.* **1995**, *36*, 297−308.

(32) Settle, R. D. F.; Rizzo, T. R. CO_2-Laser Assisted Vibrational Overtone Spectroscopy. *J. Chem. Phys.* **1992**, *97*, 2823−2825.

(33) Frisch, M. J.; Trucks, G. W.; Schlegel, H. B.; Scuseria, G. E.; Robb, M. A.; Cheeseman, J. R.; Scalmani, G.; Barone, V.; Mennucci, B.; Petersson, G. A.; et al. *Gaussian 09*; Gaussian, Inc.: Wallingford, CT, USA, 2009. See Supporting Information for full reference.

(34) Feller, D. The Role of Databases in Support of Computational Chemistry Calculations. *J. Comput. Chem.* **1996**, *17*, 1571−1586.

DOI: 10.1021/acs.jpca.5b08181
J. Phys. Chem. A 2015, 119, 10980−10987

(35) Schuchardt, K. L.; Didier, B. T.; Elsethagen, T.; Sun, L. S.; Gurumoorthi, V.; Chase, J.; Li, J.; Windus, T. L. Basis Set Exchange: A Community Database for Computational Sciences. *J. Chem. Inf. Model.* **2007**, *47*, 1045−1052.
(36) Pople, J. A.; Schlegel, H. B.; Krishnan, R.; Defrees, D. J.; Binkley, J. S.; Frisch, M. J.; Whiteside, R. A.; Hout, R. F.; Hehre, W. J. Molecular-Orbital Studies of Vibrational Frequencies. *Int. J. Quantum Chem.* **1981**, *20*, 269−278.
(37) Scott, A. P.; Radom, L. Harmonic Vibrational Frequencies: An Evaluation of Hartree-Fock, M?ller-Plesset, Quadratic Configuration Interaction, Density Functional Theory, and Semiempirical Scale Factors. *J. Phys. Chem.* **1996**, *100*, 16502−16513.
(38) Barone, V.; Biczysko, M.; Bloino, J. Fully anharmonic IR and Raman Spectra of Medium-Size Molecular Systems: Accuracy and Interpretation. *Phys. Chem. Chem. Phys.* **2014**, *16*, 1759−1787.
(39) Barone, V. Anharmonic Vibrational Properties by a Fully Automated Second-Order Perturbative Approach. *J. Chem. Phys.* **2005**, *122*, 014108.
(40) Yang, B.; Wu, R. R.; Polfer, N. C.; Berden, G.; Oomens, J.; Rodgers, M. T. IRMPD Action Spectroscopy of Alkali Metal Cation-Cytosine Complexes: Effects of Alkali Metal Cation Size on Gas Phase Conformation. *J. Am. Soc. Mass Spectrom.* **2013**, *24*, 1523−33.
(41) Armentrout, P. B.; Chen, Y.; Rodgers, M. T. Metal Cation Dependence of Interactions with Amino Acids: Bond Energies of Cs^+ to Gly, Pro, Ser, Thr, and Cys. *J. Phys. Chem. A* **2012**, *116*, 3989−3999.
(42) Dalla Via, L.; Gia, O.; Magno, S. M.; Dolmella, A.; Marton, D.; Di Noto, V. Synthesis, Characterization and Biological Activity of Platinum(II) Complexes with L- and D-Ornithine Ligands. *Inorg. Chim. Acta* **2006**, *359*, 4197−4206.
(43) Becke, A. D. Density-Functional Thermochemistry. 3. The Role of Exact Exchange. *J. Chem. Phys.* **1993**, *98*, 5648−5652.
(44) Stephens, P. J.; Devlin, F. J.; Chabalowski, C. F.; Frisch, M. J. Ab-Initio Calculation of Vibrational Absorption and Circular-Dichroism Spectra Using Density-Functional Force-Fields. *J. Phys. Chem.* **1994**, *98*, 11623−11627.
(45) Zhao, Y.; Truhlar, D. G. The M06 Suite of Density Functionals for Main Group Thermochemistry, Thermochemical Kinetics, Noncovalent Interactions, Excited States, and Transition Elements: Two New Functionals and Systematic Testing of Four M06-Class Functionals and 12 Other Functionals. *Theor. Chem. Acc.* **2008**, *120*, 215−241.
(46) Cheng, X. L.; Steele, R. P. Efficient Anharmonic Vibrational Spectroscopy for Large Molecules Using Local-Mode Coordinates. *J. Chem. Phys.* **2014**, *141*, 104105.
(47) Jaeqx, S.; Oomens, J.; Cimas, A.; Gaigeot, M. P.; Rijs, A. M. Gas-Phase Peptide Structures Unraveled by Far-IR Spectroscopy: Combining IR-UV Ion-Dip Experiments with Born-Oppenheimer Molecular Dynamics Simulations. *Angew. Chem., Int. Ed.* **2014**, *53*, 3663−3666.

DOI: 10.1021/acs.jpca.5b08181
J. Phys. Chem. A 2015, 119, 10980−10987